Technical Report

TR-13-17

LOT A2 test parcel

Compilation of copper data in the LOT A2 test parcel

Paul Wersin, Gruner Ltd.

December 2013

Svensk Kärnbränslehantering AB
Swedish Nuclear Fuel
and Waste Management Co

Box 250, SE-101 24 Stockholm
Phone +46 8 459 84 00

ISSN 1404-0344
SKB TR-13-17
ID 1403415

LOT A2 test parcel

Compilation of copper data in the LOT A2 test parcel

Paul Wersin, Gruner Ltd.

December 2013

Abstract

In the LOT A2 test parcel, compacted MX-80 bentonite blocks were exposed to temperatures up to 135°C via a central heated copper tube for a period of about five years. The main focus of this test was to study the stability of the clay under adverse conditions. Several research teams were involved in the study of the extracted core materials which is documented in a comprehensive report (Karnland et al. 2009). The analyses of the exposed clay material revealed that Cu from the metal tube had been transferred to the clay.

The scope of this contribution is to compile Cu data and to evaluate it with regard to corrosion of the Cu tube. It is to be kept in mind that the test was not designed for this purpose and thus no systematic data are available. Moreover, boundary conditions during the test were affected by complex and variable thermal, hydraulic and mechanical conditions, making clear-cut interpretation of corrosion phenomena difficult.

Analysis of five Cu profiles in the clay showed significant mass loss rates from the hot part (~ 130°C) of the Cu tube, which, converted to corrosion depths, showed an average value of 7.16 ± 3.00 μm and a median value of 8.6 μm. Assuming a constant corrosion rate during the five years of heating this would result in a median corrosion rate of 1.72 μm/a. Mass balance and other considerations point to O_2 as main corrodant, although the inventory of O_2 in the hot part is slightly lower than the Cu mass released by the hot Cu tube. Considering the total parcel and assuming that most of the initial O_2 reacted with the hot parts during the saturation process, then the mass of O_2 is calculated to be similar as the Cu mass loss. Anoxic corrosion via HS^- is not significant from a mass balance viewpoint, but it is interesting to note that Cu-rich sulphides were identified close to the Cu tube. A minor part of the Cu mass loss may be due to the leaching of oxidised Cu initially present on the surface of the Cu tube during the saturation process.

For the cold part of the Cu tube, only one profile was analysed which yields a much lower corrosion depth of 0.6 μm. There is an excess of O_2 relative to this mass loss. The calculated (average) corrosion rate (0.12 μm/a) is similar as, albeit slightly lower than, the rates deduced from three weight loss measurements of Cu coupons embedded in the clay (average value: 0.38 μm/a), and also in the same range as corrosion rates derived from two other experimental studies.

The nature of the main Cu phases resulting from the corrosion of the Cu tube has not been identified. In analogy to the observed phases on the Cu coupons, it appears reasonable, that corrosion products, such as cuprite and paratacamite, in addition to some Cu sulphides have been formed. A minor fraction of the Cu was sorbed to the clay. There are no indications of montmorillonite alteration resulting from Cu-clay interaction.

Abstract (Swedish)

I försökspaketet LOT A2 utsattes kompakterade block av MX-80 bentonit för temperaturer upp till 135°C via en central kopparvärmare under en period av ungefär fem år. Det huvudsakliga syftet med försöket var att studera lerans stabilitet under ogynnsamma förhållanden. Flera forskargrupper var involverade i studierna av testmaterialet och resultaten finns dokumenterade i en omfattande rapport (Karnland et al. 2009). Analyserna av lermaterialet visade att koppar från värmaren hade överförts till leran.

Syftet med en här studien är att sammanställa Cu data och att utvärdera dessa med avseende på korrosion av kopparröret. Det är viktigt att poängtera att detta inte var ett ursprungligt syfte med försöket och inga systematiskt framtagna data finns tillgängliga. Dessutom så har randvillkoren under försöket påverkats av de komplexa termiska, hydrauliska och mekaniska förhållandena, vilket gör entydiga tolkningar av korrosionsfenomenen svåra.

Analys av fem kopparprofiler i leran visade signifikant massförlust från den varma delen av kopparvärmaren, vilket översatt till korrosionsdjup, visade medelvärden på 7,16 ± 3.00 µm och ett medianvärde på 8.6 µm. Med förutsättning att korrosionshastigheten har varit konstant under hela den uppvärmda perioden, blir den resulterande korrosionshastigheten 1,72 µm/år (median). Massbalans och andra omständigheter pekar ut O_2 som den huvudsakliga korrodanten, dock är inventariet av O_2 i den varma delen av paketet mindre än det som motsvarar den frigjorda mängden koppar från värmaren. Om hänsyn tas till hela paketet och med förutsättning att det mesta av initial-inventariet av O_2 har reagerat med den varma delen av röret under vattenmättnadsprocessen, så överensstämmer mängden koppar och mängden syre väl. Anoxisk korrosion från HS^- är inte signifikant i ett massbalanshänseende, men det är intressant att notera att kopparrika sulfider har identifierats nära värmaren. En mindre mängd koppar kan också ha frigjorts från föroxiderat ytlager på kopparvärmaren.

I den kalla delen av kopparröret har bara en profil analyserats, vilken visade ett betydligt lägre korrosionsdjup av 0,6 µm. Det finns ett överskott av O_2 jämfört med den massförlusten. Den beräknade korrosionshastigheten (0,12 µm/år) är jämförbar, om än något lägre än hastigheten som utvärderats från viktförlustmätningar på kopparkuponger inbäddade i leran och också i samma område som korrosionshastigheter från två andra experimentella studier.

Karaktäristiken av de huvudsakliga kopparfaserna som bildats från korrosionen av kopparröret har inte identifierats. Analogt med de observerade faserna från kopparkupongerna, verkar det rimligt att korrosionsprodukter som kuprit och paratakamit, tillsammans med några kopparsulfider har bildats. En mindre andel av den frigjorda kopparn har sorberats på leran. Det finns inget som tyder på montmorillonitomvandling som följd av koppar-lera interaktion.

Contents

1 Introduction

The copper canister is the key barrier in the KBS-3 disposal concept. This is because of the inert behaviour of copper in the (reducing) host rock and near field environment and the corresponding very low predicted corrosion rates (SKB 2011). One way to support the predicted long-term behaviour is by conducting and analyzing long-term in situ tests.

The Long-term Test of Buffer Material (LOT) is an in situ experiment carried out in the Äspö Hard Rock Laboratory which focuses on the performance of the bentonite buffer and mineral stability. It comprises seven boreholes filled with doughnuts of compacted bentonite which are exposed to temperatures up to 135 ºC for different time periods (Karnland et al. 2000). These individual tests are termed test parcels.

The A2 test parcel which was extracted six years after emplacement has received particular attention. Besides the teams from SKB, teams from Andra, Nagra, Posiva and BGR participated in the analysis of the overcored materials. The work is documented in a final report (Karnland et al. 2009). In this A2 test parcel, MX-80 bentonite blocks were exposed to temperatures locally varying from 90 to 140°C for a period of about five years. The main purpose of A2 was to evaluate temperature effects on the stability of montmorillonite and on dissolution and re-precipitation of accessory minerals. The layout of the LOT A2 parcel is presented in Figure 1-1. It consisted of 38 compacted bentonite MX-80 blocks emplaced around a heated copper tube. The diameter of the borehole was 30 cm. The blocks were equipped with an array of temperature and several pressure sensors. In addition, different materials were added at different locations, e.g. cement, native copper, gypsum and K-feldspar. Heating was initiated 3 months after emplacement of the parcel in Feb. 2000. It induced a strong temperature gradient between the central heater (~ 135ºC) and the borehole wall (~ 80ºC) and also a vertical gradient at the end of the heating Cu tube, as illustrated in Figure 2-1. According to the pressure data it can be assumed that the blocks were saturated for most of the time of heat exposure, except for those very close to the heater (a few mm). From water content measurements after the test, all blocks displayed saturated conditions. The heater was switched off in December 2005. The extraction of parcel A2 was carried out in Jan. 2006. As pointed out above, several teams were involved in the sampling analysis.

The main focus of the A2 test parcel was to investigate the stability of the bentonite buffer under adverse conditions. The use of a copper tube was to study the effect of copper on the performance of the bentonite. Copper corrosion was only a side aspect which was studied with aid of emplaced coupons in the bentonite material prior to the test. This is reported by B. Rosborg in Appendix 3 of Karnland et al. (2009). The study of corrosion effects from the copper tube was not within the original focus and the experiment was not designed for this purpose. The complex boundary conditions of the heating and saturation history as well as potential galvanic coupling resulting from the metal sensors do not lend themselves for straightforward interpretation of corrosion phenomena of the copper tube. Nevertheless, some copper data in the interface area between the Cu tube and the clay were analysed. This mainly includes measurements of copper as function of distance from the heated copper metal tube, which were conducted by several laboratories.

The intention of this report is to compile all data from the A2 test parcel potentially relevant to copper corrosion. These data are then discussed and evaluated, but keeping in mind that interpretation is made difficult because of the reasons stated above.

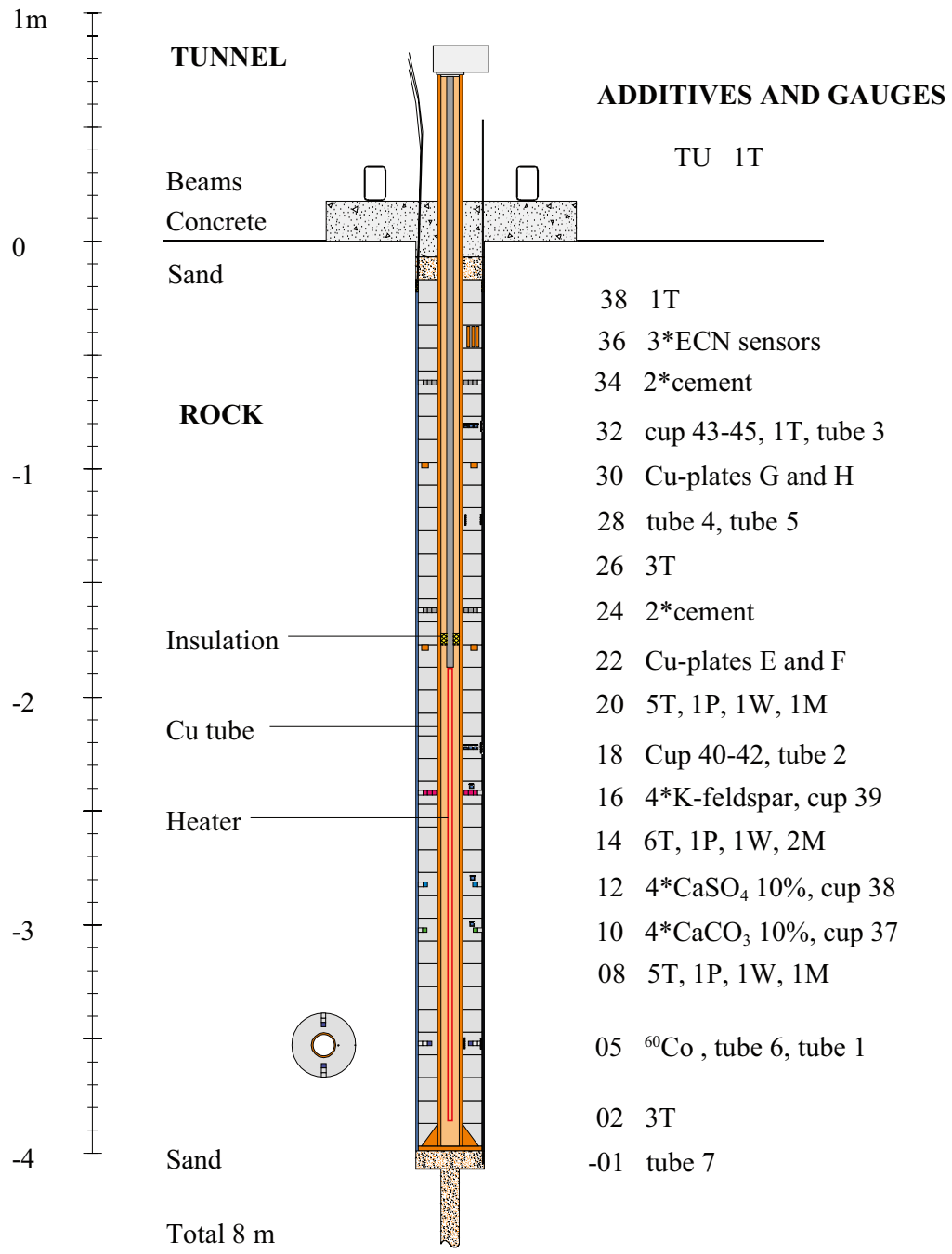

Figure 1-1. *Layout of A2 test parcel (left) and steady-state temperature distribution before cooling (right) (Karnland et al. 2009, Figure 3-3).*

2 Data compilation

2.1 Copper-related work in the LOT A2 test parcel

Several teams analysed the copper in the clay as function of distance from the heated copper tube. The locations of the different profiles analysed in the test parcel are illustrated in Figure 2-1. Moreover, copper coupons emplaced in two locations were analysed after extraction of the core (also shown in Figure 2-1). The different analyses performed by the different organisations are summarised in Figure 2-1.

Clay Technology (Clay Tech)

This team analysed two profiles (blocks 09 & 11) in the hot area and one in the cold area (block 33). The slicing and segmentation of the blocks are illustrated in Figure 2-2. The slice thickness of the samples perpendicular to the Cu tube was about 2 cm. After drying at 60°C, major and trace elements of the bulk and of the <2 micron fractions were analysed with ICP-AES and ICP-MS. Exchangeable cations of bulk materials were analysed by extraction into an alcoholic ammonium chloride solution. Cation exchange capacity (CEC) was determined by the Cu(II) triethylenetetramine method. Method details are presented in Chapter 9 of Karnland et al. (2009).

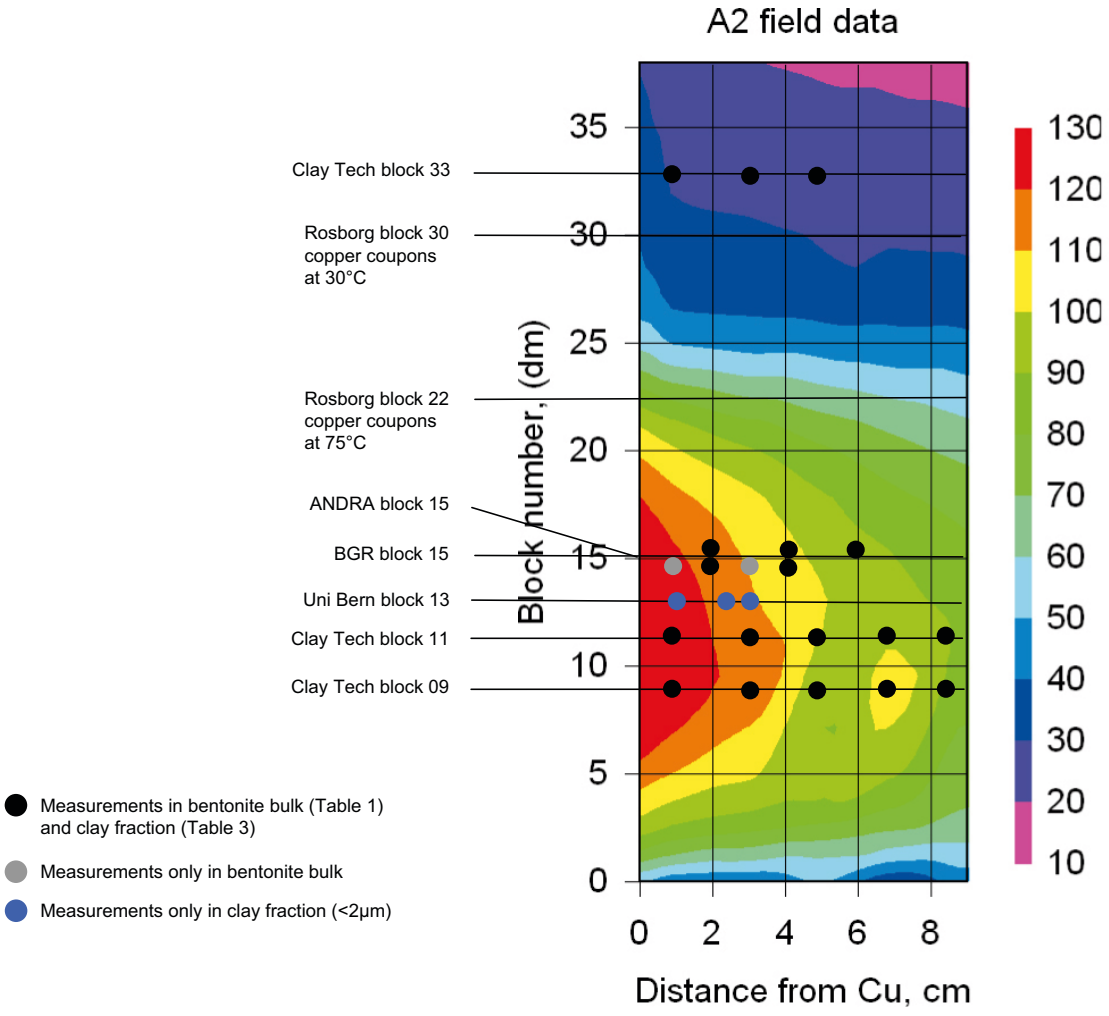

Figure 2-1. *Examined additive-free blocks and temperature distribution in the parcel at termination of the heating (Karnland et al. 2009, Figure 4-4). Scale on right hand side refers to temperature in °C.*

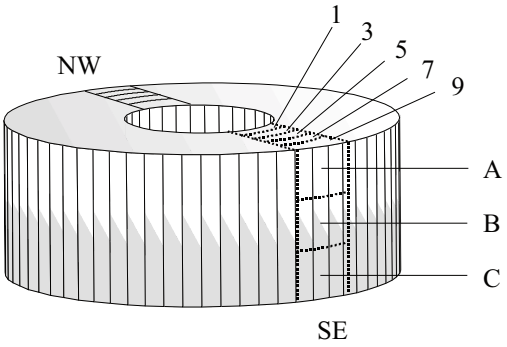

Figure 2-2. *Preparation of clay samples by Clay Tech (Karnland et al. 2009, Figure 3-2). Schematic block partition. SE and NW denote the directions of compass in the test-hole, figures denote the centre of the spectimens expressed in centimeters measured from the block inner mantel surface, and A, B and C denotes the analyzed three vertical position in the blocks.*

ANDRA

The team involved was the Ecole Nationale Supérieure de Géologie in Nancy (F). One profile (block 15) in the hot area was analysed for major and trace elements by ICP-AES and ICP-MS. The slice thickness was about 2 cm (Figure 2-3). Both bulk and the <2 micron fractions were analysed. In addition, one fragment located at the interface to the Cu tube was embedded in resin and analysed with SEM. Small isolated particles (~ 5 µm) of the same sample were further measured by TEM to increase the spatial resolution. Finally, a small fragment of the interface was also analysed with XPS. Method details are presented in Appendix 6 of the LOT report.

BGR

The team of BGR analysed two profiles (block 15) in the hot area with XRF after drying samples at 60°C. The width was 1 cm for the innermost slice and 2 cm for subsequent slices (Figure 2-4). Also, in situ m-EDXRF measurements were performed on one of the profiles which yielded relative intensity information. In addition, the surface of the block in direct contact with the Cu tube was studied with light microscopy which revealed a bluish metallic grain of about 10 µm. This phase was further analysed with SEM. Method details are presented in Appendix 7 of the LOT report.

Uni Bern

Within the work of Uni Bern there was little focus on the copper aspect. The only Cu analysis was that of exchangeable cations obtained from the nickel ethylenediamine method. Method details are presented in Appendix 8 of the LOT report.

B. Rosborg

Four copper coupons (60 × 15 × 1.5 mm) were placed in the warm (~ 75°) block 22 and the cold (~ 30°) block 30 before the test. The scope was to determine nature and extent of copper corrosion by analysing the materials after the test. The analyses included weight loss measurements, microscopy and XRD of the coupons and (semiquantitative) SEM-EDX analysis of one profile in the clay. Method details are presented in Appendix 3 of the LOT report.

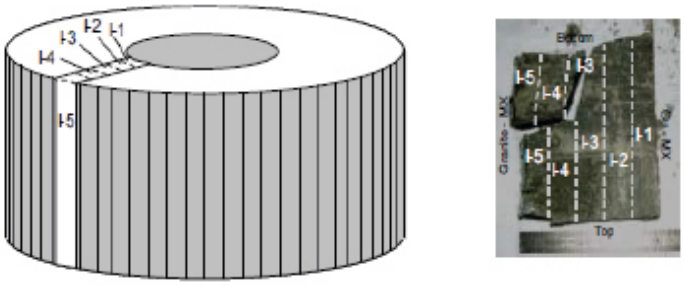

Figure 2-3. *Preparation of clay samples by ANDRA team (Karnland et al. 2009, Figure A6-3). Five samples have been collected from the LOT A2/15 slide #1. Each sample is ca 2 × 2 × 10 cm (L × W × H) and are labelled from 1 to 5 according to the distance from the copper-MX80 interface (Sample 1 is the nearest).*

Figure 2-4. *Preparation of clay samples by BGR (Karnland et al. 2009, Figure A7-1).*

2.2 Initial conditions of the Cu tube

As indicated in the introduction, the description of the A2 test parcel, including materials, preparation, installation and heating procedures, is described in Karnland et al. (2009). Of interest here are the initial conditions of the Cu tube surrounding the central heater (Figure 2-1). The Cu tube is made of SS 5015-04 alias CW024A and termed Cu-DHP. It is de-oxidised pure copper (Cu ³ 99.9 wt–%) with a limited content of phosphorus (0.015–0.04 wt–%) (Deutsches Kupferinstitut 2013). This material can be expected to be nearly exempt of any oxidised surface film. In contact with air, a thin (nanometer range) protective oxidised surface film (Cu_2O and CuO) forms (Speckmann et al. 1985).

The Cu tube had a shiny surface and only minor signs of corrosion when received at the laboratory of Clay Technology (Karnland O 2013, personal communication). The Cu tube was put in contact with the moist bentonite blocks during preparation of the parcel. It was then transported from Lund to the Äspö HRL and emplaced in the test hole at the end of October 1999. At that time the surface had become slightly darker (O. Karnland, pers. communication). Heating was started about three months later (February 2, 2000) and perfomed in steps of 10°C until the final power of 850 W was reached. Water supply was initiated simultaneously in the slot between the clay column and the rock.

It can be deduced from this information that the initial amount of oxidised Cu on the surface of the tube induced by the oxidation in air is not known but likely to be small. This point is briefly discussed in section 3.2.

2.3 Copper mass losses

2.3.1 Copper profiles in bulk material

Copper concentrations as function of distance from the heated Cu tube were analysed in the bulk material by three laboratories (Clay Tech, Andra, BGR). The data are reported for blocks (10 cm high doughnuts). The results of five profiles from hot blocks and one profile from a cold block are shown in Table 2-1. These give a fairly consistent picture with regard to five calculated Cu mass losses from the Cu tube and corresponding corrosion depths for the hot blocks. The averaged mass loss is 2.18 ± 0.91 g (1σ)[1] per block (median 2.61 g) which, normalized to the Cu surface, yields an average corrosion depth of 7.16 ± 3.00 µm and a median of 8.58 µm. For cold blocks, only one profile (Clay Tech) was analysed. The derived mass loss is considerably lower –0.18 g per block, which yields a corrosion depth of 0.60 µm, thus roughly a factor of ten lower.

Table 2-1. Measured Cu concentration in bentonite bulk as function of distance from copper heater.

	Sample#	Cu conc.	max. distance to Cu	volume (h: 10 cm)	mass bentonite per block section	mass Cu transferred per block section	tot.corr depth	av. corrrate (5a)
		ppm	cm	cm3	kg	g	µm	µm/a
Clay Tech block 09 hot	A209BW1b	2325	2	804.2	1.26	2.93	9.64	1.93
	A209BW3b	5	4					
	A209BW3b-2	5	4					
	A209BW5b	5	6					
	A209BW7b	5	8					
	A209BW9b [a]	5	10					
	av. mass Cu corroded					2.93	9.64	1.93
Clay Tech block 11 hot	A211BW1b	1600	2	804.2	1.26	2.02	6.63	1.33
	A211BW3b	6	4	1055.6	1.66	0.003	0.01	0.002
	A211BW5b	4	6					
	A211BW7b	4	8					
	A211BW9b [a]	4	10					
	av. mass Cu corroded					2.02	6.65	1.33
ANDRA block 15 hot	15 I1 RT	2110	2	804.2	1.26	2.66	8.75	1.75
	16 I2 RT	9	4	1055.6	1.66	0.01	0.02	0.00
	17 I3 RT	6.1	6	1306.9	2.05	0.003	0.01	0.00
	Reference	4.47						
	av. mass Cu corroded					2.67	8.79	1.76
BGR block 15 hot ("1st block")	1 cm	4075	1	370.7	0.58	2.37	7.80	1.56
(1st mm sample omitted)	2 cm	240	2	433.5	0.68	0.16	0.53	0.11
	4 cm	50	4	1055.6	1.66	0.08	0.25	0.05
	Reference	4						
	av. mass Cu corroded					2.61	8.58	1.72
BGR block 15 hot ("2nd block")	1 cm	1053	1	370.7	0.58	0.61	2.01	0.40
(1st mm sample omitted)	2 cm	62	2	433.5	0.68	0.04	0.13	0.03
	3 cm	12	3	496.4	0.78	0.01	0.02	0.00
	Reference	4						
	av. mass Cu corroded					0.66	2.16	0.43
Average hot blocks 5 profiles	CT09, CT11, Andra15, BGR15-1, BGR15-2							
Arithmetic mean						2.18	7.16	1.43
Median						2.61	8.58	1.72
Standard-Deviation						0.91	3.00	0.60
Clay Tech block 33 cold	A233BW1b	149	2	804.2	1.26	0.18	0.60	0.12
	A233BW3b	4	4					
	A233BW5b	4	6					
	A233BW7b [a]	4	8					
	A233BW9b [b]	162	10					
	av. mass Cu corroded					0.18	0.60	0.12

[a] Used as reference sample to subtract background Cu.

[b] the higher Cu concentration in this sample is explained by presence of thermocouple tubing in Karnland et al. (2009).

[1] 1σ also applies to the following standard deviations.

Corrosion estimates on copper coupons placed in the warm (~ 75°C) block 22 and the cold (~ 30°C) block 30 by weight loss measurements were carried out by Bo Rosborg (LOT report Appendix 3). As highlighted by the author, the coupons in block 22 were damaged by the cutting wheel during the retrieval, thus making accurate measurements impossible (see p. 147). Nevertheless, an attempt to estimate corrosion rates from weight loss measurements was made for one sample in this block. The Cu mass losses for the coupons (~ 20 cm^2) were estimated to be 31 mg, 46 mg, and 27 mg for samples A22E, A30g, A30H respectively. This leads to corresponding corrosion depths of 1.7 µm, 2.52 µm and 1.48 µm. It should be noted that the uncertainty in boundary conditions in such types of measurements is rather large.

The Cu exchangeable by NH_4^+ extraction was also analysed in the bulk fraction, together with the other cations Na^+, Ca^{2+}, Mg^{2+} and K^+. The corresponding concentrations are listed in Table 2-2. This shows that Cu could be detected only in the innermost section in contact with the Cu tube. The extracted amount of Cu varied from 0–3 meq/kg. Thus, only a minor fraction of the total Cu (max. 6%) occurs as exchangeable cation (compare Table 2-1 and Table 2-2). The main exchangeable cation in samples was found to be Na^+, followed by Ca^{2+} and Mg^{2+}.

2.3.2 Copper profiles in clay fraction

Copper in the less than 2 µm fraction was determined by two labs (Clay Tech and Andra). The separation was done by centrifuged sedimentation. Four profiles were analysed, as depicted in Table 2-3. The calculated mass losses from the two Clay Tech profiles are 0.78 and 0.55 g Cu per block, corresponding to 27% of the Cu mass obtained for the corresponding bulk material. The Cu content analysed in the Andra profile was considerably larger: 1.55 g Cu corresponding to 58% of Cu mass relative to that of the bulk.

The SEM-EDX analysis carried out by the ANDRA teams showed no enrichment towards the Cu tube, which is not in line with the chemical analyses. The reason for this mismatch is unclear.

The profile from the cold block analysed by Clay Tech shows a Cu mass loss of 0.27 g per block which is higher than that obtained from the corresponding bulk material (0.18 g). The reason for this unexpected result may lie in the extraction procedure of the clay particle fraction which may have induced some ion exchange reaction.

The extractable Cu via the Ni-en method was analysed in one hot profile by Uni Bern. The extracted Cu concentration is much lower than the (total) Cu concentrations in the clay fraction obtained by Clay Tech and Andra. This is in line with the results of Clay Tech on the bulk material (section 2.2.1) which also indicate that only a small fraction of the Cu is in the exchangeable fraction.

Table 2-2. Cations extracted by NH_4^+ in bentonite bulk fraction (meq/kg).

	Sample#	Na	K	Ca	Mg	Cu	fraction of Cu_{tot}
		meql/kg	meql/kg	meql/kg	meql/kg	meql/kg	%
Clay Tech block 09 hot	A209BW1b	456	11	172	85	2	3%
	A209BW3b	486	13	175	85	0	
	A209BW5b	515	14	174	82	0	
	A209BW7b	548	13	171	80	0	
	A209BW9b	517	12	158	75	0	
Clay Tech block 11 hot	A211BW1b	463	12	182	83	3	6%
	A211BW3b	476	12	176	76	0	
	A211BW5b	481	12	165	73	0	
	A211BW7b	513	12	158	70	0	
	A211BW9b	490	11	153	66	0	
Clay Tech block 33 cold	A233BW1b	492	12	163	55	0	0%
	A233BW3b	528	13	176	53	0	
	A233BW5b	508	14	166	52	0	
	A233BW7b	491	12	164	51	0	
	A233BW9b	504	11	160	50	0	

Table 2-3. Cu concentrations in clay fraction (< 2 mm) as function of distance from copper heater.

	Sample#	Cu conc.	distance to Cu	mass Cu transferred per block section	total Cu per block [b]	fraction of total Cu (%)	Comments
		ppm	cm	g			
Clay Tech block 09 hot	A209BS1c	642	2	0.78			
	A209BS3c	27	4				
	A209BS5c	24	6				
	A209BS7c	24	8				
	A209BS9c [a]	25	10				
	av. mass Cu corroded			0.78	2.93	26.59	
Clay Tech block 11 hot	A211BW1c	479	2	0.55			
	A211BW3c	5	4				
	A211BW5c	5	6				
	A211BW7c	17	8				
	A211BW9c [a]	44	10				
	av. mass Cu corroded			0.55	2.02	27.21	
Clay Tech block 33 cold	A233BS1c	241	2	0.27			
	A233BS3c	15	4				
	A233BS5c	42	6				
	A233BS7c	40	8				
	A233BS9c [a]	28	10				
	av. mass Cu corroded			0.27	0.18	146.90	see text
ANDRA block 15 hot	15 I1 2u	1229	2	1.55			see text
	16 I2 2u	8	4	0.004			
	17 I3 2u	5.96	6				
	Reference	5.8					
	av. mass Cu corroded			1.55	2.67	58.00	
		meq/100g					
Uni Bern block 13	Ni W1-B 0.5/1	1.64	1.2	0.07			
(Ni-en exctraction)	Ni W-2B 0.5/1	0.015	2.4				
	Ni W-3B 0.5/1	0.015	3				
	Reference	0.015					
	av. mass corroded			0.07			

[a] Used as reference sample to subtract background Cu.

[b] taken from Table 2-1.

2.4 Corroding agents

O_2

Under aerobic conditions, Cu is corroded by the interaction with molecular O_2 leading to Cu(II) species, schematically represented by:

$$Cu + ½\ O_2 + 2H^+ \rightarrow Cu^{2+} + H_2O \quad (1)$$

The generated Cu(II) may further react with Cu, leading to Cu(I) species:

$$½Cu^{2+} + ½Cu \rightarrow Cu^+ \quad (2)$$

The main final corrosion products via this corrosion process are, depending on solution conditions, $Cu(I)_2O$ (cuprite), $Cu(II)Cl_2 \times 3Cu(II)(OH)_2$, Cu(II) hydroxycarbonate (malachite, azurite) and sorbed Cu(II) (King et al. 2002).

In terms of mass balance, this means that 0.5 mole O_2 are required to corrode 1 mole Cu(0) to 1 mole Cu(II) while only 0.25 mole O_2 are required for the corrosion to 1 mole Cu(I).

The initial inventory of molecular O_2 in the LOT borehole can be calculated from the air content in three compartments: the inner gap between the Cu surface and the inner block surface (2 mm), the air-filled porosity in the blocks and the outer gap between the outer block surface and the borehole wall (10.7 mm). The O_2 inventory is calculated from the initial geometric configuration in the bore-hole and accounting for the initial solid-water mass ratio (0.1), the grain density (2.75 Mg/m^3), the (designed) wet density (2.00 Mg/m^3), the density of air (1.25 mg/m^3) and the O_2 mass fraction in

air (23.135%). Thus, the calculation yields 0.02 g (inner gap), 0.175 g (initial block) and 0.28 g (outer gap) of O_2 present. The derived O_2 inventories per block (height 10 cm) for the three compartments are shown in Table 2-4.

The outer slot was initially water filled and therefore we consider only the remaining initial O_2, i.e. in the bentonite blocks and the inner gap between block and Cu to be available for corrosion of the Cu tube. As shown in Table 2-4, this yields an inventory of 0.195 g or 6.09 mmole per block.

Fe(III)

A further potential oxidant is Fe(III) in the bentonite. As revealed from analysis of the bulk and clay fraction, virtually all Fe is contained in the clay fraction (see Karnland et al. 2009, Tables 9-5 and 9-6). Assuming that all the total Fe in the clay is present as structural Fe(III) one obtains an upper amount for this species. Structural Fe(III) might be an oxidant for Cu(0) although, so far no experimental data is available to support this hypothesis. The potential corrosion process is schematically represented by:

$$Cu + Fe(III)–clay \rightarrow Cu(I) + Fe(II)–clay \quad (3)$$

This reduction process in the clay leads to an increase in layer charge and CEC. The oxidant is part of the solid and thus this process, if occurring at all, is restricted to the interface between the Cu surface and the bentonite. It should be pointed out, however, that the extent of such a redox process is affected by the electrical conduction properties in bentonite which are poorly known.

For a mass balance estimate we consider that the redox process occurs in the first cm of the Cu-bentonite contact area. This choice is somewhat arbitrary and supporting experimental data are lacking. As depicted in Table 2-4, the mass of structural Fe(III) in the first cm is estimated to be 6.0 g or 0.11 mole of Fe(III). It has been derived from the mean Fe values reported by Clay Tech in Table 9-6 of Karnland et al. (2009).

Note that the CEC increase from Fe(III) reduction, assuming that no side reactions occur (e.g. precipitation of Fe(II)), is directly related to the mole Fe(III) reduced: The CEC in 1 cm of block is 0.37 eq. Thus, if all Fe(III) were reduced to Fe(II) an increase to 0.48 eq. or 30% would result. CEC data from Clay Tech suggests an increase with CEC for the hot area (Karnland et al. 2009, Table 9-5), which is about 5% compared to the cold area. Hence, this increase, if related to Fe(III) reduction, would have affected only part of structural Fe(III). It should be pointed out that the increase of CEC close to the heater indicated by Clay Tech measurements was not confirmed by the studies of the other labs (BGR, Andra and Uni Bern). An uncertainty in this regard is the possible re-oxidation of reduced Fe(II) during the experimental procedure of CEC analysis. This may have "erased" the higher CEC in the samples contacting the Cu source.

In summary, the reduction of structural Fe(III) in contact with Cu is not more than a hypothesis with no experimental data to confirm this redox process. Because of its interfacial character, only the clay in the contact region is likely to be affected. Assuming 1 cm of clay in the contact region to have reacted with the Cu tube, then a maximum of 100 mmole Fe(III) per block could oxidize the equivalent amount of Cu. This would induce a CEC increase of 30% which however is not in line with measured data. These suggest that CEC increase is much lower, although these data might have been affected by re-oxidation effects.

HS^-

Under anoxic conditions, dissolved sulphide is the main corroding agent for Cu (e.g. King et al. 2002) which supports the cathodic reaction with water leading to the precipitation of Cu_2S, schematically represented as:

$$2Cu + HS^- + H^+ \rightarrow Cu_2S + H_2 \quad (4)$$

As proposed by several authors (e.g. Wersin et al. 1994, Smith et al. 2007), Cu corrosion in compacted bentonite is directly related to the HS^- flux from the surrounding groundwater. For the LOT A2 test, this flux is not straightforward to evaluate because of the complex boundary conditions. For estimating this flux, two different cases are assumed. For the first case, a steady-state flux of HS^- (F_{HS}) through the bentonite with a pessimistically selected constant concentration at the borehole interface C_{HS} of 10^{-5} mole/L is assumed. According to Fick's 1st law of diffusion, the steady-state HS– flux F_{HS} is:

$$F_{HS} = D_e \times \varepsilon \times \Delta C/\Delta X \quad (5)$$

where D_e is the effective diffusion coefficient, e is the porosity of the buffer (0.43), $\Delta C \approx C_{HS}$ and ΔX is the diffusion distance taken to be 0.048 m (½ of block thickness). For the cold blocks, the effective diffusion coefficient of HS^- in the bentonite is taken to be 2.3×10^{-12} m^2/s (King 2002). This leads to a HS^- flux of 2.06×10^{-13} mole/m^2/s and to the 4.12×10^{-13} mole/m^2/s of Cu corroded according to equations (4) and (5). The calculated corrosion depth for an assumed five years of anoxic corrosion is 4.62×10^{-4} µm. For hot blocks, the diffusivity of HS^- is a factor of about 30 higher (King et al. 1997), thus leading to a total corroded depth of 0.014 µm. The second case assumes mixing of the porewater volume per block (0.43×6.15 L = 2.64 L) with groundwater displaying a HS^- concentration of 10^{-5} mole/L. This results in 2.64×10^{-5} mole HS^- which, according to eq. (4), would corrode 5.28×10^{-5} mole Cu and lead to a corroded depth of about 0.01 µm after five years.

Table 2-4. Calculated masses of Cu, O_2, Fe(III), and HS^- per block (see text).

	mass per block (g)	mass per block (mole)	equiv. mass for Cu(I) (mole)	equiv. mass for Cu(II) (mole)	max. equiv. corrosion depth (µm)
1. Copper					
hot blocks					
average mass lost 5 profiles	2.18	3.43E-02			7.16
median mass lost 5 profiles	2.61	4.10E-02			8.58
cold blocks					
mass lost (1 profile)	0.18	2.88E-03			0.60
2. Oxygen					
mass inner gap	1.99E-02	6.23E-04	2.49E-03	1.25E-03	0.52
mass init. block	1.75E-01	5.46E-03	2.19E-02	1.09E-02	4.57
mass outer gap	2.81E-01	8.77E-03			
total O_2 inventory	4.75E-01	1.49E-02			
inventory available for corrosion (see text)	1.95E-01	6.09E-03	2.43E-02	1.22E-02	5.09
3. Fe(III)					
mass 1st cm	6.0	1.09E-01	1.09E-01	5.45E-02	22.77
(CEC 1st cm)		3.73E-01			
4. HS^- from groundwater					
a) steady-state diffusion (5yr)					
- hot blocks		3.32E-05	6.63E-05	3.32E-05	0.014
- cold blocks		1.11E-06	2.21E-06	1.11E-06	4.62E-04
b) mixing with groundwater		2.64E-05	5.27E-05	2.64E-05	0.011

Other sulphur sources:

Pyrite may occur as impurity in MX-80. According to Karnland et al. (2006) its content is 0.24%. In the presence of O_2 at circumneutral pH pyrite is unstable and oxidizes to Fe(III) oxyhydroxide and sulphate. Thus under aerobic conditions, it is unlikely that pyrite in the clay contributes to Cu corrosion; rather the opposite, by consuming part of the O_2 in the near field (e.g. Wersin et al. 1994, Grandia et al. 2006). Under anaerobic conditions, on the other hand, pyrite is very insoluble over a wide range of conditions and the release of HS^- is very low. Thus, the sulphide flux generated is negligible compared to that assumed for the surrounding groundwater (see above).

A large sulphur source is obviously the sulphate pool from gypsum in the clay and from the groundwater (Karnland et al. 2009). Sulphate may act as electron acceptor under reducing conditions in the presence of sulphate reducing bacteria (SRB). Under compacted saturated conditions, microbial activity is inhibited by the low water activity and high swelling pressure of the clay (Stroes-Gascoyne et al. 2007, Pedersen 2000). It should be pointed out that there is still some uncertainty regarding the possibility of SRB activity in compacted bentonite, as suggested by the recent study of Masurat et al. (2010). In that study, the rate of sulphide increased with decreasing density; at a saturated density of 2000 kg/m^3, an equivalent copper corrosion rate of 1.8×10^{-4} µm/a was determined.

A further potential sulphur source is MoS_2 contained in the lubricant applied in block manufacturing (O. Karnland, personal communication). The quantity thereof is unknown. This compound however is very insoluble over a wide range of conditions and thus the release of sulphide is low.

2.5 Mass balance considerations

2.5.1 Oxygen

Hot blocks

The masses of corroding agents can be compared to the Cu mass losses (Table 2-4). This comparison shows that for the hot blocks the O_2 inventory available for corrosion is slightly lower than the Cu mass transferred from the hot Cu tube. Thus, the median value of 41 mmole of corroded Cu compares with 6.1 mmole of O_2. From eq. (1) and (2), an amount of about 10–20 mmole O_2 would be required to oxidize this amount of Cu.

Cold blocks

The analogous comparison exercise with the cold block shows that there is an excess mass of oxygen available to oxidize the measured mass loss of 0.18 g or 20.5 mmole Cu.

Total parcel

From the saturation history it can be envisioned that the gaseous O_2 initially present in the borehole does not react homogeneously with the Cu tube. As stated above, the outer slot was initially water filled. Karnland et al. (Chapter 9, LOT report) proposed that the residual air from the unsaturated parts was pushed to the hot areas which were the last to saturate. Hence, it is of interest to check O_2 mass balance for the whole test parcel with a length of 4 m. From Figure 2-1 the hot area (>110°C) next to the heater corresponds to about 1.20 m and the cold area (<50°C) to about 1.60 m. This leaves 1.2 m for the warm part (50–110°C). For the hot area, the median corrosion depth is 8.58 µm. For the cold part, the corrosion depth is estimated from one Cu profile (0.6 µm) (Table 2-1) and the average from two weight loss measurements of a coupon placed in the cold part (2.0 µm) yielding 1.3 µm. For the remaining warm part, the mass loss is estimated to be twice of that for the cold part, yielding a corrosion depth of 2.6 µm. Using these corrosion depths, results in Cu mass loss of 47.15 g Cu or 0.74 mole (Table 2-5). The calculated mass of O_2 available for Cu corrosion in the parcel is 7.8 g or 0.24 mole. This gives an equivalent oxidant mass for Cu(I) of 0.97 mole. Thus, in principle sufficient O_2 on a parcel basis is available to explain the mass loss from the Cu tube.

Table 2-5. Calculated masses of Cu and O_2 per total parcel, (see text).

	total corrosion depth (μm)	mass per block (g)	repres. height (m)	represen. mass per parcel (g)	represen. mass per parcel (mole)	equiv. mass for Cu(I) (mole)
1. Copper						
hot blocks (5 profiles)	8.58	2.61	1.20	31.30	0.49	
warm blocks (guess)	2.61	0.79	1.20	9.51	0.15	
cold blocks (1 profile CT+ av Rosborg)	1.30	0.40	1.60	6.34	0.10	
total Cu of parcel			4.00	47.15	**0.74**	
2. Oxygen						
total mass available for corrosion		0.19	4.00	7.79	0.24	**0.97**

2.5.2 Other potential corrodants

Fe(III)

As depicted from Table 2-4, the amount of structural Fe(III) in a 1 cm thick clay slice of a block adjacent to the Cu tube is about 0.11 mole. This amount would be sufficient to explain the mass loss. However, as pointed out above, the reduction of structural Fe(IIII) is not supported by CEC data which suggest that the mass of reduced Fe(III) would be at maximum 0.02 mole.

HS^-

As pointed out above, the HS^- originating from the groundwater is far too low to explain the copper mass loss rates. The microbially induced reduction of sulphate in the vicinity of the Cu tube under conditions of the test is highly unlikely, because of the high compaction and resulting low water activity and subsequent high swelling pressure of the clay. The direct reduction of sulphate by Cu metal is thermodynamically not feasible (Grauer 1990). The release of sulphide from pyrite is very low owing to the very low solubility of this phase under reducing conditions. The same statement holds for MoS_2 contained in the applied lubricant, whose quantity in the bentonite block is not known.

2.6 Solid phase data

As summarised in section 2.1, the clay material close to the Cu tube was analysed within the contribution of the Andra and BGR teams. These teams also investigated the Cu phases in the contact area. Copper coupons placed inside the clay were analysed by Bo Rosborg.

2.6.1 Results from Andra

The Andra team analysed samples with SEM, TEM and XPS. The main findings from SEM was, besides of newly formed $CaSO_4$, the identification of small particles (~ 5 μm) enriched in Cu and sulphur and variable content of Fe close to the Cu source. An example of a Cu sulphide precipitate enriched in Fe analysed by SEM-EDX is shown in Figure 2-5.

These phases were further analysed by TEM-EDX which indicated three different types of sulphide particles: (i) high Fe content in the centre and Cu-S enriched at the rims, (ii) medium Fe content and evenly distributed Cu and S, Fe appears correlated with the O content; interpreted as mixture of Cu sulphide and Fe oxide and (iii) low Fe content with Cu sulphide particles.

A further small fragment at the interface was analysed by XPS in a qualitative manner, thus probing the uppermost ~ 5 nm of the surface. From the results, the authors suggest the occurrence of Cu with sulphides and oxides, but the data appear to be rather uncertain.

From the overall analysis, the authors conclude that Cu at the interface occurs likely as small particles of sulphide and oxide, and that it has not "reacted directly with the phyllosilicates" although acknowledging that the analysis is preliminary. They further tentatively suggest that destabilization of primary minerals pyrite and carbonates have led to the precipitation of Ca sulphates, Cu sulphides and Fe oxides.

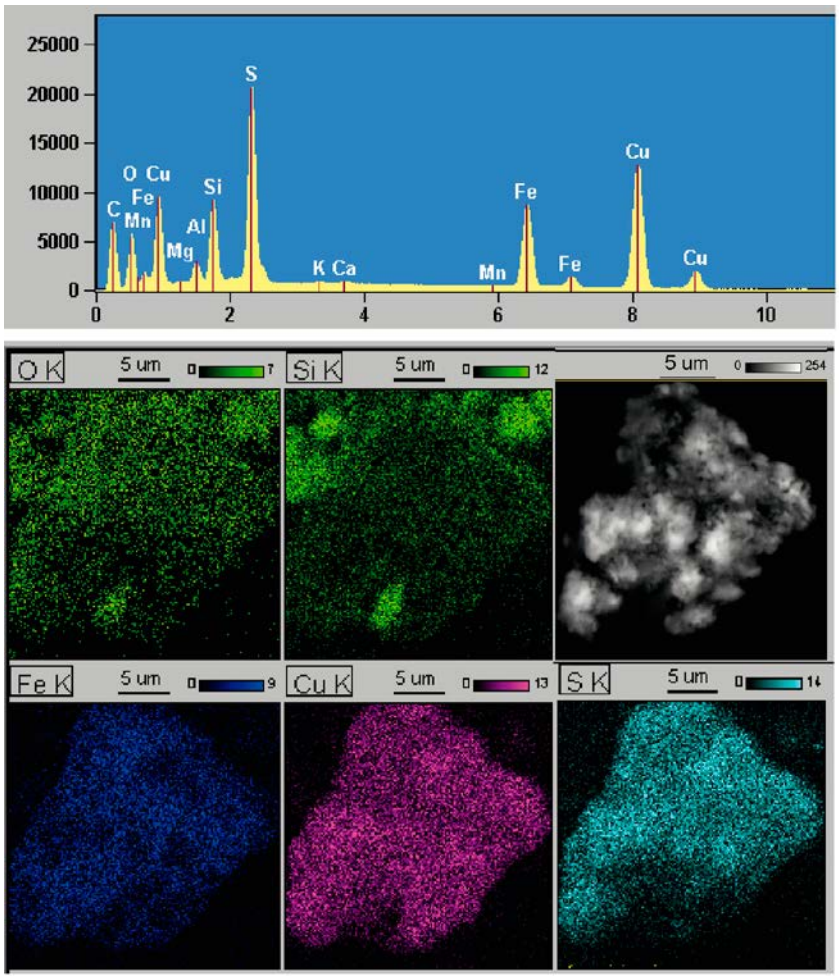

Figure 2-5. *SEM-EDX pattern of Cu-rich phase at contact Cu-bentonite (Karnland et al. 2009, Figure A6-11). Note the almost missing oxygen peak.*

2.6.2 Results from BGR

The surface of the bentonite block in direct contact with the Cu tube was analysed by light and electron microscopy. A bluish phase was detected in contact with (probably newly formed) calcite crystals (Figure 2-6). From combined results, it was proposed that the identified Cu rich particle (~ 5 µm diameter) represents a Cu sulphide. Furthermore, the authors suggested that these Cu sulphides have formed from reduction of sulphates triggered by Cu corrosion.

2.6.3 Results from B. Rosborg

The corrosion products on the surface of the clay after breaking loose the clay from the Cu coupon A230 were analysed. A brownish corrosion product layer on the bentonite underlain by a blue-green one was observed (Figure 2-7). XRD measurements indicated that the main brown phase was cuprite ($Cu(I)_2O$) and the blue-green one was para-atacamite ($Cu(I)_2(OH)_3Cl$) (Figure 2-8).

2.6.4 Summary evaluation

Preliminary microscopic and spectroscopic analysis of the (heated) clay adjacent to the Cu tube indicates the formation of Cu-rich sulphide grains with varying amount of Fe and possibly also $CuSO_4$. No Cu association with silicate phases was detected. Whether in addition also Cu oxide phases, typical corrosion products from oxic Cu corrosion, were formed at the Cu tube surface, could not be clarified. Cuprite and para-atacamite corrosion products however were identified at the Cu coupons surfaces placed in the colder parts of the clay.

The frequent association of Cu with Fe and S suggests interaction of released Cu from the tube with primary pyrite from the clay. The amount of pyrite in MX-80 is about 0.24% (Karnland et al. 2006). Considering that most of the Cu lost from the Cu tube is in the first cm and is about 0.3 mole per block, it is interesting to compare this amount with that of available pyrite in that volume. This is calculated to be 0.01 mole of pyrite or 0.02 mole of sulphur. Thus, this amount is not sufficient to bind all of the Cu. This simple mass balance suggests that most of the Cu released from the Cu tube is not present as sulphide. It is worth noting that natural pyrites contain variable amounts of Cu (Abraitis et al. 2004). It is not obvious from the study of Andra and BGR what the Cu content of the pyrites further away from Cu tube is. The above calculation represents thus a maximum estimate of Cu originating from the Cu tube. A further uncertainty related to this consideration is the possible presence of MoS_2-containing lubricant applied in the experiment (see sections 2.3 and 3.2). However the effect thereof is expected to be small because of the very low solubility of MoS_2.

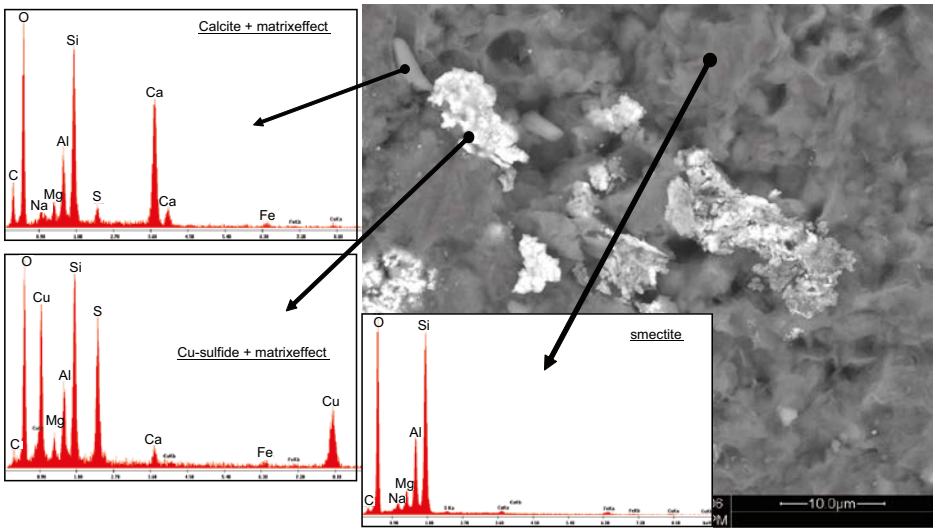

Figure 2-6. *SEM-EDX pattern of clay matrix and Cu-rich phase close to Cu tube (Karnland et al. 2009, Figure A7-17).*

Figure 2-7. *Corrosion products of Cu coupon (Karnland et al. 2009, Figure A3-1a). In upper part corrosion coupon is in place. Brownish corrosion product is cuprite (Cu_2O).*

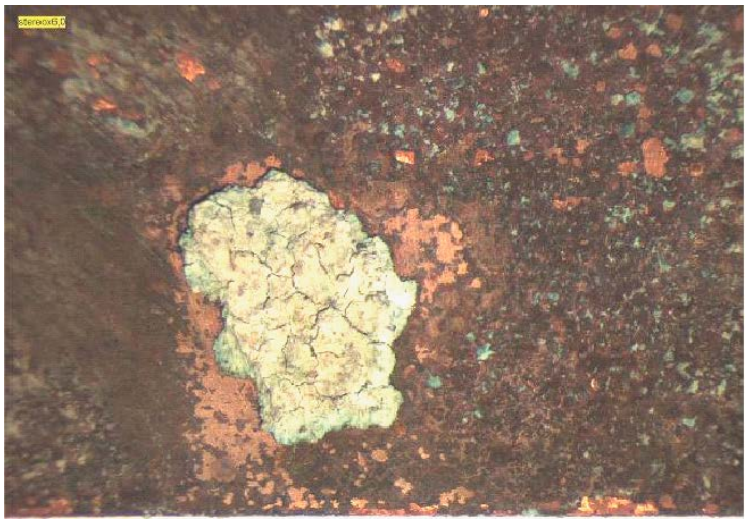

Figure 2-8. *Corrosion products of Cu coupon (Karnland et al. 2009, Figure A3-1c). Blue-green corrosion products (almost white in picture) identified as para-atacamite ($Cu_2(OH)_3Cl$).*

3 Discussion

3.1 Corrosion rates

The obtained corrosion rate estimated from LOT A2 can be compared to other reported Cu corrosion rates in compacted bentonite, as shown in Table 3-1. In the study of Kumpulainen et al. (2010), compacted saturated MX-80 in Cu vessels was reacted with 0.5 M NaCl solutions in N_2 atmosphere at room temperature for more than 8 years. Cu corrosion rates were estimated from three Cu profiles in the clay perpendicular to the Cu vessel surface. The estimated corrosion rate was 0.04 µm/a. Kim et al. (2007) studied the corrosion of small Cu rods embedded in compacted Ca bentonite contacted with synthetic groundwaters in Ar atmosphere as function of time at 70°C up to 3.4 years. The obtained corrosion rates showed a slight decrease with time, for the longest period a corrosion rate of about 0.6 µm/a was determined. Cuprite (Cu_2O) was observed as corrosion product. Both studies reflect "mixed" redox conditions, thus initially oxic and then anoxic conditions. A comparison with the corrosion rates estimated from the LOT A2 test parcel shows that the rates from the colder sections fall in the range of the two reported studies, but those from the hot region are clearly higher. They fall within the upper range of oxic corrosion rates derived from a steady state box model of Wersin et al. (1994) (Table 3-1). It should be highlighted however, that these high rates observed in LOT were observed in the hot clay, whereas all other rates were derived from colder conditions.

The corrosion rates under anoxic conditions are expected to be much lower because of the thermodynamic stability of Cu metal. In model approaches (e.g. Wersin et al. 1994, King et al. 2002), the corrosion rate is taken to be directly related to the HS^- flux. Applying this approach to the LOT A2 test parcel and assuming a HS^- concentration of 10^{-5} M as boundary condition at the clay/rock interface, less than 1 nm/a are estimated for the "cold" Cu tube, and about 3 nm/a for the hot tube (Table 2-4). The difference is related to the higher diffusion rate at high temperature.

3.2 Corrosion process and corrosion products

The corrosion process of the hot Cu tube cannot be unequivocally unravelled. This is partly due to the incomplete data, especially with regard to the solid phase and partly due to the complex boundary conditions. The rather high mass losses clearly point to O_2 as main corrodant. From a mass balance viewpoint, the inventory of O_2 in the hot part is slightly lower than the Cu mass lost from the metal tube. Considering the whole parcel and assuming the majority of O_2 during the saturation process has been "pushed" towards the hot Cu tube and consumed there at a faster rate than at the colder parts, then the amount of O_2 corresponds about to the Cu mass loss. However, this would imply that almost all of the O_2 initially present in the borehole would have reacted with the hot Cu tube, and other redox active species such as Fe(II) and pyrite in the clay would have contributed much less to O_2 consumption.

Table 3-1. Comparison of Cu corrosion rates in compacted bentonite derived from different studies.

Study	corrosion time (a)	total corrosion depth (µm)	corrosion rate (µm/a)	Comments
LOT A2 Cu_tube	5	8.58	1.72	130°C, median 5 profiles
LOT A2 Cu_tube	5	0.60	0.12	30°C, median 1 profile
LOT A2 Cu coupon	5	1.90	0.38	30;60°C, average 3 samples
Kumpulainen et al.	8.2	0.31	0.04	20°C, average 3 samples
Kim et al.	variable	variable	0.60	70°C, average 4 samples
Hallberg et al.	1.E+05	1500	0.015	bronze cannon in clay sediment
Wersin et al.			0.007–7	steady-state oxic corr. model
Wersin et al.			5E-5–0.004	steady-state HS^- corr. model

In the above considerations, the oxidised Cu initially present has been neglected. As pointed out in section 2.2, this amount is likely to be small due to the presence of a protective thin copper oxide surface film and the observation of a predominantly shiny surface. Assuming that a uniform oxidised surface film composed of Cu_2O of 1 µm thickness was leached during the experiment, a mass loss of Cu of 0.18 g for a 10 cm block would result. This would correspond to about 8% of the total average mass loss in the hot part. This is considered to correspond to a maximum estimate since the average surface film thickness is likely to be smaller.

From the solid phase analysis of the hot area, separate Cu-rich sulphide and possibly also $CuSO_4$ grains were identified. Based on their analysis, the Andra team also proposed the occurrence of Cu-containing oxide phase, whose nature however could not be identified. No Cu bound to silicates was detected. The amount of primary sulphide (pyrite) is too low to explain all Cu present at the hot Cu tube/bentonite interface. On the other hand, MoS_2-containing lubricant was applied in bentonite block manufacturing (see sections above), which might have also been a sulphur source for Cu sulphide compounds. MoS_2 is difficult to detect with "standard" EDX because of strong overlap of Mo and S peaks (Piburn and Barron 2012), thus this phase might not have been detected in the SEM-EDX analysis conducted by the Andra and BGR teams. However, as pointed out above, MoS_2 is very insoluble and therefore not a significant sulphide source. Mass balance considerations suggest that non-detected Cu corrosion products under aerobic conditions were formed in the Cu tube-clay contact area. It needs to be noted that the microscopic and spectroscopic analysis must be regarded as preliminary.

For the colder parts, fewer data are available. But these show a rather consistent picture in terms of corrosion rates and corrosion products. The identified corrosion products on the surface of the Cu coupons embedded in the clay are cuprite and para-atacamite, which both form under oxic to suboxic conditions.

3.3 Copper-clay interaction

Besides forming corrosion products, corroded Cu may in principle react with the montmorillonitic clay by sorption (cation exchange, sorption to edge sites) or copper silicate precipitation (King and Wersin 2013). As presented in section 2.2, the amount of exchangeable Cu is small compared to the total Cu in the bentonite contacting the Cu tube (a few % of the total Cu). This was shown by two extraction techniques (NH_4^+ and Ni^{2+}) applied by two different lab teams (Clay Tech and Uni Bern). Hence, the major Cu pool in the clay next to the Cu tube is most likely made of Cu precipitates.

The solid phase analysis performed by the Andra and BGR teams showed no indication of Cu silicate phases. The formation of such phases, such as chrysocolla ($CuSiO_3 \times 2H_2O$) as alteration products of native copper is rare and restricted to specific geochemical conditions (oxidising, high silica and low carbonate activities) (King and Wersin 2013).

From the above considerations, it is deduced that Cu-clay interaction led to some sorbed Cu, but most likely not to any Cu silicate phases. Most of the Cu in the clay at the metal contact is present as separate corrosion products. These findings also indicate that the stability of montmorillonite was not affected by the Cu corrosion process.

4 Conclusions

Copper data from the LOT A2 test parcel have been compiled and analysed. The main focus thereby has been to evaluate corrosion phenomena of the heated Cu tube in contact with the MX-80 blocks. No unambiguous picture could be obtained, which is not surprising since the test was not designed for this purpose and thus no systematic data are available. Nevertheless, some interesting features can be noted:

- From the five Cu profiles perpendicular to the Cu tube, corrosion rates can be estimated. For the hot blocks, the calculated median corrosion depth is 8.6 µm which yields a corrosion rate of 1.7 µm/a. For the cold part of the Cu tube, one Cu profile yields a much lower corrosion rate of 0.12 µm/a, which is similar to the rate estimated from weight loss of copper coupons. It is also in the same range as reported corrosion rates from two experimental studies.
- Mass balance and other considerations point to O_2 as main corrodant, although the inventory of O_2 in the hot part is slightly lower than the Cu mass released by the hot Cu tube. Considering the total parcel and assuming that most of the initial O_2 in the borehole reacted migrated to the hot parts during the saturation process and rapidly reacted with the Cu surface, then the mass of O_2 is calculated to be similar as the Cu mass loss.
- From a mass balance viewpoint, structural Fe(III) in the clay might have contributed to the mass loss of the Cu tube, but from CEC data and the lack of evidence in the literature, there is not much support for such a corrosion process.
- The mass of HS^- originating from the surrounding groundwater or from dissolution of sulphide minerals is clearly too low to explain the copper released from the Cu tube. A part of the Cu however has reacted with sulphur and Cu-rich sulphide has formed at the interface of the hot Cu tube. A potential sulphide source, besides pyrite, is MoS_2 contained in the lubricant. Microbially-induced sulphate reduction is inhibited or at least strongly limited in compacted bentonitic clay and therefore is not considered relevant under test conditions.
- Dissolution of the initially oxidised Cu on the surface of the Cu tube and transfer to the clay during the saturation process may have contributed to Cu mass loss, but this contribution is expected to be rather small, presumably less than 8% of the total Cu transferred to the clay.
- The nature of the corrosion product(s) other than Cu sulphide (and possibly $CuSO_4$) around the Cu tube has not been identified. In analogy to the observed phases on the Cu coupons, it appears reasonable, that corrosion products, such as cuprite and paratacamite have been formed.
- The interaction between the Cu released from the corrosion process and the montmorillonite remained limited. A minor fraction of the Cu was sorbed to the clay. There are no indications of montmorillonite alteration resulting from Cu-clay interaction.

Acknowledgements

We would like to thank Fraser King, Lawrence Johnson, Ola Karnland and Patrik Sellin for fruitful discussions. The comments of Christina Lilja, Ola Karnland, Daniel Svensson and Allan Hedin have significantly helped to improve this manuscript.

References

SKB's (Svensk Kärnbränslehantering AB) publications can be found at www.skb.se/publications.

Abraitis P K, Pattrick R A D, Vaughan D J, 2004. Variations in the compositional, textural and electrical properties of natural pyrite: a review. International Journal of Mineral Processing 74, 41–59.

Deutsches Kupferinstitut, 2013. Cu-DHP. Düsseldorf: Deutsches Kupferinstitut. Available at: http://www.kupferinstitut.de/front_frame/pdf/Cu-DHP.pdf

Grandia F, Domènech C, Arcos D, Duro L, 2006. Assessment of the oxygen consumption in the backfill. Geochemical modelling in a saturated backfill. SKB R-06-106, Svensk Kärnbränslehantering AB.

Grauer R, 1990. The reducibility of sulphuric acid and sulphate in aqueous solution. PSI-Bericht Nr. 109, Paul Scherrer Institute, Switzerland, SKB TR 91-39, Svensk Kärnbränslehantering AB.

Hallberg R O, Östlund P, Wadsten T, 1988. Inferences from a corrosion study of a bronze cannon, applied to high level nuclear waste disposal. Applied Geochemistry 3, 273–280.

Karnland O, Sandén T, Johannesson L-E, Eriksen T E, Jansson M, Wold S, Pedersen K, Motamedi M, Rosborg B, 2000. Long term test of buffer material. Final report on the pilot parcels. SKB TR-00-22, Svensk Kärnbränslehantering AB.

Karnland O, Olsson S, Nilsson U, 2006. Mineralogy and sealing properties of various bentonites and smectite-rich clay materials. SKB TR-06-30, Svensk Kärnbränslehantering AB.

Karnland O, Olsson S, Dueck A, Birgersson M, Nilsson U, Hernan-Hakansson T, Pedersen K, Nilsson S, Eriksen T E, Rosborg B, 2009. Long term test of buffer material at the Äspö Hard Rock Laboratory, LOT project. Final report on the A2 test parcel. SKB TR-09-29, Svensk Kärnbränslehantering AB.

Kim S S, Chun K S, Kang K C, Baik M H, Kwon S H, Choi J W, 2007. Estimation of the corrosion thickness of a disposal container for high-level radioactive wastes in a wet bentonite. Journal of Industrial and Engineering Chemistry 13, 959–964.

King F, 2002. Corrosion of copper in alkaline chloride environments. SKB TR-02-25, Svensk Kärnbränslehantering AB.

King F, Wersin P, 2013. Review of supercontainer copper shell-bentonite interactions and possible effects on buffer performance for the KBS-3H design. Posiva Working Report 2013-03, Posiva Oy, Finland.

King F, Ryan S R, Litke C D, 1997. The corrosion of copper in compacted clay. AECL 11831, COG-97-319-I, Pinawa, Manitoba, Canada: Whiteshell Laboratories.

King F, Ahonen L, Taxén C, Vuorinen U, Werme L, 2002. Copper corrosion under expected conditions in a deep geologic repository. Posiva 2002-01, Posiva Oy, Finland.

Kumpulainen S, Kiviranta L, Carlsson T, Muurinen A, Svensson D, Sasamoto H,Yui M, Wersin P, Rosch D, 2010. Long-term alteration of bentonite in the presence of metallic iron. SKB R-10-52, Svensk Kärnbränslehantering AB, Posiva Working Report 2010-71, Posiva Oy, Finland.

Masurat P, Eriksson S, Pedersen K, 2010. Microbial sulphide production in compacted Wyoming bentonite MX-80 under *in situ* conditions relevant to a repository for high-level radioactive waste. Applied Clay Science 47, 58–64.

Pedersen K, 2000. Microbial processes in radioactive waste disposal. SKB TR-00-04, Svensk Kärnbränslehantering AB.

Piburn G, Barron A R, 2012. An introduction to energy dispersive X-ray spectroscopy. Connexions Web site. Available at: http://cnx.org/content/m43555/1.1/ [29 May 2012].

SKB, 2011. Long-term safety for the final repository for spent nuclear fuel at Forsmark. Main report of the SR-Site project. SKB TR-11-01, Svensk Kärnbränslehantering AB.

Smith J, Qin Z, King F, Werme L, Shoesmith D W, 2007. Sulphide film formation on copper under electrochemical and natural corrosion conditions. Corrosion 63, 135–144.

Speckmann H-D, Lohrengel M M, Schultze J W, Strehblow H-H, 1985. The growth and reduction of duplex oxide films on copper. Berichte der Bunsengesellschaft für physikalische Chemie 89, 392–402.

Stroes-Gascoyne S, Hamon C J, Dixon D A, Kohle C, Maak P, 2007. The effects of dry density and porewater salinity on the physical and microbiological characteristics of compacted 100% bentonite. In Dunn D, Poinssot C, Begg B (eds). Scientific basis for nuclear waste management XXX: symposium held in Boston, Massachusetts, USA, 27 November – 1 December 2006. Warrendale, PA: Materials Research Society. (Materials Research Society Symposium Proceedings 985), paper 0985-NN13-02.

Wersin P, Spahiu K, Bruno J, 1994. Kinetic modelling of bentonite–canister interaction. Long-term predictions of copper canister corrosion under oxic and anoxic conditions. SKB TR 94-25, Svensk Kärnbränslehantering AB.